Soret and Dufour effects in entropy optimized mixed convective flow of Carreau-Yasuda fluid: A numerical study

Wei-Feng Xia[1], M. Ijaz Khan[2,*], Faris Alzahrani[3], Aatef Hobiny[3]

[1]School of Engineering, Huzhou University, Huzhou 313000, P. R. China

[2]Department of Mathematics, Riphah International University, Faisalabad Campus, Faisalabad 38000, Pakistan

[3]Nonlinear Analysis and Applied Mathematics (NAAM)-Research Group, Department of Mathematics, Faculty of Sciences, King Abdulaziz University, P.O. Box 80203, Jeddah 21589, Saudi Arabia

(Corresponding author email: mikhan@math.qau.edu.pk (M. Ijaz Khan))

Abstract: This research communication reports a computational study of mixed convection towards a stretched surface with a Carreau-Yasuda model (non-Newtonian fluid). A Carreau-Yasuda model, acceptable for numerous non-Newtonian models, is utilized to illustrate the behavior of both shear thinking and thinning liquids. The energy and concentration equations are developed using the concept of law of conservations of energy and mass in the presence of thermal radiation, Soret and Dufour effects, viscous dissipation and activation energy. Total entropy rate depends on four different types of irreversibilities, i.e., thermal, Joule heating, fluid friction, mass and calculated through second law of thermodynamics. Convective boundary conditions is imposed at the boundary for both heat and mass transport. The governing equations are transformed into ordinary ones via appropriate similarity transformations and numerical results are obtained through Built-in-Shooting method. The pertinent flow parameters for the problem are mixed convection parameter, Soret and Dufour parameters and activation parameter. The impact to the constitutive non-Newtonian fluid (Carreau-Yasuda model) on the velocity, temperature,

concentration, entropy generation rate, skin friction and heat transfer rate is discussed in detail. The obtained results are compared with previous published research articles and good agreement is found. The results reveal that temperature increases against higher values of Dufour parameters.

Keywords: Carreau Yasuda fluid; Convective conditions; Soret and Dufour effects; Entropy generation; Mixed convection; Activation energy

1: Introduction

The obliged capitalization of impressively organized fluids has persuaded remarkable attentiveness of present research community. In the recent few couple of years various examination on these multifaceted natured liquid have been initiated because of their significant and valuable pertinence in many procedures i.e., food emulsions, friction reduction, biopolymer systems, cooling by surfactants and many others [1-3]. Therefore, researchers and investigators have recommended the essentialness of liquids in various procedures. But with the improvement in time and change in different mechanical and industrial technological processes are happing so it is exceptionally significant to create such liquids which adapt up to them. Therefore, experts of fluid dynamics have proposed numerous non-Newtonian fluid models in this regards after analyzing the behavior and demand of required progressions. To anticipate the rheological attributes of shear thinning liquids which has utilize in manufacturing of multiple emulsions and polymerization, various models for example Ellis model [4], Ostwald-de-Waele model [5], Williamson model [6], Cross model [7], Carreau-Yasuda model [8] and Carreau model [9] are proposed. Among the above fluid models, the Carreau-Yasuda model has obtained inescapable consideration of researchers and investigators because of its adequate behavior for the narrative of shear thinning liquid. Carreau-Yasuda model is the generalized form of power law model. The power law model depends on a two parameter i.e., k and n whereas Carreau-Yasuda model is depends on five

parameter model i.e., $(\eta_0, \eta_\infty, n, a, \lambda)$. Andrade [10] worked on Kolmogorov dissipative scales and skin friction equation for turbulent pipes flow using Carreau-Yasuda fluid model In this research, he discussed the turbulent flow behavior of Carreau-Yasuda model and skin friction equation is derived assuming a logarithmic impact of turbulent velocity towards the near wall flow out of the viscous sub layer. They obtained results are also compared experimentally with methyl hydroxil cellulose solutions and found good agreement. Some important and influential studies in regards of non-Newtonian materials can be seen in Refs. [11-17].

Stretching surfaces play an important role in industrial applications such as fiber glass production, wire drawing and hot rolling etc. Sakiadis [18] studied the boundary layer assumptions on a solid sheet surface moving with uniform speed. In this study, he concentrate on the boundary layer flow of continuous solid surfaces and basic differential and integral momentum expressions of boundary layer theory are derived for these surfaces. Furthermore, the derived differential and integral momentum expressions are solved for both laminar and turbulent flow. Crane [19] pioneered the work by presenting exact solution for two dimensional steady stretching flow problems. Many authors extended the work of Crane by studying different aspects of the stretching flow problem [20-21]. Rashid et al. [22] scrutinized radiated flow of non-Newtonian fluid (thixotropic fluid) with chemical reaction towards a stretched surface. They discussed the flow behavior over a stretched surface and generated by linear stretching velocity. The derived flow expressions are solved analytically through semi analytical method (Optimal Homotopy Analysis Method (OHAM)). Total residual errors for the velocity, temperature and concentration equations are calculated. Hsiao [23] analyzed incompressible, steady electrical conducting dissipative free convective flow of Maxwell fluid near a stagnation point towards a stretched surface. The governing flow expressions are first converted into ordinary ones and then tackled by an improved

numerical finite difference method. Further attempts in the boundary layer area with stretching sheet phenomenon can be observed in Refs. [24-32].

The efficient consumption of energy and resources have highly motivated the researchers to improve he efficiencies in industrial processes. Analysis of heat transfer is considered as the key factor in consumption of energy. Entropy optimization with different types of non-Newtonian fluids is an important tool for getting maximum heat transfer rate. New advancements and better efficiencies in industries and engineering processes have been achieved by using entropy generation. Bejan started the work on entropy minimization [33]. This concept is mainly based on 2nd law of thermodynamics. Recently much attempts have been done in this area taking different geometries. Second law of thermodynamics is used by Rashidi et al. [34] considering incompressible flow of electrically conducting fluid over a rotating disk with magnetic field effects. Electrically conducting fluid is considered and the analysis is carried out by a stretched surface of disk. They claim that the considered flow has a applications in thermal conversion mechanisms for nuclear propulsion space vehicles and MHD energy generators. Through implementation of second of thermodynamics total entropy rate is calculated and the results are compared with published articles in the literatures and found good agreement with them. Further, Rashidi et al. [35], Malvandi et al. [36] and Soraya and Salah [37] worked on entropy optimized MHD stretched flow of viscous material for both heat and mass transport in the presence of magnetohydrodynamic, nanofluid, slip effects, porosity and variable fluid properties.

In this work, entropy generation rate is studied in flow of non-Newtonian fluid (Carreau-Yasuda fluid) towards a stretched surface with mixed convection. Both energy and concentration equations are developed in the presence of thermal radiation, Soret and Dufour effects, viscous dissipation, chemical reaction and activation energy. Total entropy rate is discussed. Convective boundary

conditions is imposed at the boundary for both heat and mass transport. The impact of influential flow parameters are discussed on the velocity, concentration, temperature, skin friction, entropy generation rate and Nusselt number. The governing equations are solved numerically via Built-in-Shooting method and results are compared with other techniques and found very good analysis with them.

2: Theoretical formulation

2.1: Problem statement

Here we considered two-dimensional steady-incompressible mixed convective flow of Carreau-Yasuda fluid towards a stretched surface. The flow is generated due to linear stretching velocity i.e., $u = ax$, where a denotes the stretching rate or dimensional constant. Thermal radiation, Soret and Dufour effects, viscous dissipation, activation energy and chemical reaction effects are utilized in the mathematical modeling of energy and concentration equations. At the boundary of stretched surface $u = ax$ highlights the stretched velocity in $x-$ direction, $v = 0$ denotes there is no suction/injection at the boundary, $-k\frac{\partial T}{\partial y} = h_f\left(T - T_\infty\right)$, $-D_c\frac{\partial C}{\partial y} = h_c\left(C - C_\infty\right)$ represent the convective conditions for both heat and mass transport, where k indicates the thermal conductivity, h_f the heat transfer coefficient, T the temperature, h_c the mass transfer coefficient, T_∞ the ambient temperature, C the concentration, D_c the mass diffusion and C_∞ the ambient concentration. The schematic geometry of the problem is illustrated in Fig. 1. In 1972, the rheological expressions of Carreau fluid is initially derived by Carreau [16] and broadly has been utilized up to date. The constitutive expression of [16] for incompressible flow is addressed as

$$\boldsymbol{\tau} = 2\mu\left(\gamma^*\right)D^*, \tag{1}$$

where $\mu\left(\gamma^*\right)$ is defined as

$$\mu\left(\gamma^*\right)=\left[\mu_\infty+\left(\mu_0-\mu_\infty\right)\left(1+\left(\Gamma\gamma^*\right)^2\right)^{\frac{n-1}{2}}\right]. \tag{2}$$

In Eq. (2), γ^* indicates the shear rate and addressed as

$$\gamma^*=\sqrt{2D^*\ :\ D^*}. \tag{3}$$

The model [16] is further improved in 1979 by Yasuda [17]:

$$\mu\left(\gamma^*\right)=\left[\mu_\infty+\left(\mu_0-\mu_\infty\right)\left(1+\left(\Gamma\gamma^*\right)^d\right)^{\frac{n-1}{d}}\right]. \tag{4}$$

Note that, μ_∞ indicates the viscosity at infinite shear rate, μ_0 viscosity at zero shear rate, Γ stands for time constant and n the power law index. It is also note that the above model predicts the Newtonian behavior, pseudoplastic fluid and dilatant fluid respectively for $n=1,\ n<1$ and $n>1$. Also, a special case i.e., Newtonian fluid can be achieved by letting $n=1$ or $\Gamma=0$.

2.2: Dimensional equations

The dimensional equations i.e., the continuity, momentum, energy and concentration in the presence of applied flow assumptions are defined as [8, 38, 39, 40]:

$$\frac{\partial u}{\partial x}+\frac{\partial v}{\partial y}=0, \tag{5}$$

$$\left.\begin{aligned} u\frac{\partial u}{\partial x}+v\frac{\partial u}{\partial y}=\nu\frac{\partial^2 u}{\partial y^2}+\Gamma^d\nu\left(\frac{n-1}{d}\right)(d+1)\frac{\partial^2 u}{\partial y^2}\left(\frac{\partial u}{\partial y}\right)^d \\ -\frac{\sigma B_0^2}{\rho}u+g\left[\beta_t\left(T-T_\infty\right)+\beta_c\left(C-C_\infty\right)\right], \end{aligned}\right\} \tag{6}$$

$$\left.\begin{aligned} u\frac{\partial T}{\partial x}+v\frac{\partial T}{\partial y}=\frac{k}{\rho c_p}\frac{\partial^2 T}{\partial y^2}+\frac{\mu_0}{\left(\rho c_p\right)}\left(\frac{\partial u}{\partial y}\right)^2+\frac{\mu_0}{\left(\rho c_p\right)}\left(\frac{n-1}{d}\right)\Gamma^d\left(\frac{\partial u}{\partial y}\right)^2\left(\frac{\partial u}{\partial y}\right)^d \\ +\frac{16\sigma^* T_\infty^3}{3k^*}\frac{\partial^2 T}{\partial y^2}+\frac{D_c k_T}{c_s c_p}\frac{\partial^2 C}{\partial y^2}, \end{aligned}\right\} \tag{7}$$

$$u\frac{\partial C}{\partial x}+v\frac{\partial C}{\partial y}=D_c\frac{\partial^2 C}{\partial y^2}+\left(\frac{D_c k_T}{T_m}\right)\frac{\partial^2 T}{\partial y^2}-k_r^2\left(C-C_\infty\right)\left(\frac{T}{T_\infty}\right)^m \exp\left[\frac{-E_a}{\kappa T}\right], \tag{8}$$

with

$$\left.\begin{aligned} u=ax,\ v=0,\ -k\tfrac{\partial T}{\partial y}=h_f\left(T-T_\infty\right),\ -D_c\tfrac{\partial C}{\partial y}=h_c\left(C-C_\infty\right) \quad \text{at} \quad y=0,\\ u\to 0,\ T\to T_\infty, C\to C_\infty \quad \text{when} \quad y\to\infty. \end{aligned}\right\} \tag{9}$$

Note that, Eq. (5) is the continuity equation which physical means that the influx is always equal to the outflux in the absence of any source/sink, Eq. (6) is the momentum equation which physical means that the total momentum of the body always remain conserved, where first term of the L. H. S. represents the inertial forces, the first term of R. H. S. represents the viscous forces, the second term is due to fluid model and the third term is due to the mixed convection, Eq. (7) is the energy equation which physical means that the total energy of the body remain conserved, where the first term of the L. H. S. indicates the internal energy, the first term of the R. H. S. is due to the conduction, the second term is due to the dissipative energy, the third term is due to the radiative heat flux and the last term is due to the Dufour effect, Eq. (8) is the law of conservation of mass which physically means the total mass of the mass is always conversed, where the first term of the L. H. S. and R. H. S. is due to the Fick's first law, the second term is due to the Soret effect, the third term is due to the chemical reaction and activation energy. In Eq. (8), the surface of the stretching sheet is represented at $y=0,$ i.e., $y=0$ highlights the stretched surface of sheet and $y\to\infty$ highlights the surface away from the stretched surface.

In the above expressions, u,v indicates the velocity components in $x-$ and $y-$ respectively, ν the kinematic viscosity, g the gravity acceleration, β_t,β_c the thermal and concentration expansions coefficients, ρ the density, c_p the specific heat, k the thermal conductivity, μ_0 the dynamic viscosity, σ^* the Stefan-Boltzman constant, k_r the reaction rate, k^* mean absorption

coefficient, m the fitted rate constant, E_a the coefficient of activation energy and $\kappa = 8.61\times10^{-5} eV/K$ the Boltzman constant porosity rate, k_T the thermal mean temperature, c_s the concentration susceptibility and T_m the fluid mean temperature.

Let us consider the following appropriate transformations

$$\eta = y\sqrt{\frac{a}{\nu}},\ u = axf'(\eta),\ v = -\sqrt{a\nu}\,f(\eta),\ \theta(\eta) = \frac{T-T_\infty}{T_w-T_\infty},\ \phi(\eta) = \frac{C-C_\infty}{C_w-C_\infty}. \tag{10}$$

We arrive at

$$f''' + (We)^d \frac{(n-1)(d+1)}{d} f'''(f'')^d + \lambda\theta + N\lambda\phi - f'^2 + ff'' - \beta_1 f' = 0, \tag{11}$$

$$\theta'' + \Pr Ecf''^2\left(1+\frac{n-1}{d}(We)^d(f'')^d\right) + \Pr f\theta' + D_f \Pr \phi'' + R\theta'' = 0, \tag{12}$$

$$\phi'' + LeSr\theta'' + Lef\phi' - Le(1+\delta\theta)^m k_1 \exp\left[\frac{-E_1}{(1+\delta\theta)}\right] = 0, \tag{13}$$

$$\left.\begin{aligned} f(0)=0,\quad f'(0)=1,\quad f'(\infty)\to 0,\quad \theta'(0) = -B_1(1-\theta(0)),\\ \phi'(0) = -B_2(1-\phi(0)),\quad \theta(\infty)\to 0,\ \phi(\infty)\to 0, \end{aligned}\right\} \tag{14}$$

where $We\left(=\Gamma x\sqrt{\frac{a^3}{\nu}}\right)$ denotes the Weissenberg number, $Gr_x\left(=\frac{g\beta_T(T_w-T_\infty)}{\nu^2}x^3\right)$ the Grashof number, $N\left(=\frac{\beta_c(C_w-C_\infty)}{\beta_T(T_w-T_\infty)}\right)$ the buoyancy ratio parameter, $\mathrm{Re}_x\left(=\frac{Ux}{\nu}=\frac{ax^2}{\nu}\right)$ Reynolds number, $\lambda\left(=\frac{Gr_x}{\mathrm{Re}_x^2}\right)$ mixed convection parameter, $D_f\left(=\frac{D_c k_T(C_w-C_\infty)}{C_s C_p(T_w-T_\infty)\nu}\right)$ the Dufour number, $\Pr\left(=\frac{(\rho c_p)\nu}{k}\right)$ the Prandtl number, $Ec\left(=\frac{(ax)^2}{c_p(T_w-T_\infty)}\right)$ the Eckert number, $Sr\left(=\frac{D_c k_T(T_w-T_\infty)}{T_w(C_w-C_\infty)\nu}\right)$ the Soret number, $Le\left(=\frac{\nu}{D_c}\right)$ the Lewis number, $R\left(=\frac{16\sigma^* T_\infty^3}{3kk^*}\right)$ the radiation parameter, $E_1\left(=\frac{E_a}{\kappa T_\infty}\right)$ the activation energy parameter, $k_1\left(=\frac{k_r^2}{a}\right)$ the chemical reaction parameter, $B_1\left(=\frac{h_f}{k}\sqrt{\frac{\nu}{a}}\right)$ the thermal Biot number, $\beta_1\left(=\frac{\sigma B_0^2}{\rho a}\right)$ the magnetic

parameter, $B_2\left(=\frac{h_c}{D_c}\sqrt{\frac{\nu}{a}}\right)$ the solutal Biot number, $Sc\left(=\frac{\nu}{D_c}\right)$ the Schmidt number and $\delta\left(=\frac{T_w-T_\infty}{T_\infty}\right)$ the temperature ratio parameter.

3: Modeling of entropy

The volumetric entropy equation for the Carreau-Yasuda fluid model in the presence of radiative heat flux, viscous dissipation and concentration is defined as

$$S_G=\underbrace{\frac{k}{T_\infty^2}\left[\left(\frac{\partial T}{\partial y}\right)^2+\frac{16\sigma^* T_\infty^3}{3kk^*}\left(\frac{\partial T}{\partial y}\right)^2\right]}_{\text{Thermal irreversibility}}+\underbrace{\frac{\mu_0}{T_\infty}\left[\left(\frac{\partial u}{\partial y}\right)^2+\frac{n-1}{d}\Gamma^d\left(\frac{\partial u}{\partial y}\right)^2\left(\frac{\partial u}{\partial y}\right)^d\right]}_{\text{Fluid friction irreversibility}}$$
$$+\underbrace{\frac{R^*D}{T_\infty}\left(\frac{\partial T}{\partial y}\frac{\partial C}{\partial y}\right)+\frac{R^*D}{C_\infty}\left(\frac{\partial C}{\partial y}\right)^2}_{\text{Concentration irreversibility}}+\underbrace{\frac{\sigma B_0^2}{T_\infty}u^2}_{\text{Joule heating irreversibility}}. \tag{15}$$

After implementing the Eq. (10), the dimensionless form is

$$N_G=(R+\delta)\theta'^2+Br\left(f''^2+\frac{n-1}{d}(We)^d\left(f''\right)^d f''^2\right)+\beta_1 Brf'^2+L\theta'\phi'+\frac{L\alpha_2}{\delta}\phi'^2, \tag{16}$$

where $\alpha_2\left(=\frac{C_w-C_\infty}{C_\infty}\right)$, $L\left(=\frac{R^*D(C_w-C_\infty)}{k}\right)$, $Br\left(=\frac{\mu a^2x^2}{k\Delta T}\right)$ and $N_G\left(=\frac{S_G T_\infty \nu}{ak\Delta T}\right)$ respectively denote the concentration ratio parameter, diffusion parameter, Brinkman number and entropy generation rate. The Bejan number is addressed as

$$Be=\frac{\text{Heat transfer irreversibility+Mass transfer irreversibility}}{\text{Total entropy}}, \tag{17}$$

$$Be=\frac{(R+\delta)\theta'^2+L\theta'\phi'+\frac{L\alpha_2}{\delta}\phi'^2}{N_G}, \tag{18}$$

4: Physical quantities

The skin friction coefficient and Nusselt number for the Carreau-Yasuda fluid is addressed as

$$C_f = \frac{\tau_w}{\rho(u_w)^2},\ Nu = \frac{xq_w}{k(T_w - T_\infty)}, \tag{19}$$

where τ_w and q_w respectively highlight the shear stress and heat flux and is defined as

$$\left.\begin{aligned} \tau_w &= (\tau_{zr})_{z=0} = \mu_0\left[\left(1+\Gamma^d\left(\tfrac{n-1}{d}\right)\left(\tfrac{\partial u}{\partial y}\right)^d\right)\left(\tfrac{\partial u}{\partial y}\right)\right]_{y=0} \\ q_w &= \left[-k\left(\tfrac{\partial T}{\partial y}\right)\right]_{y=0} + \text{thermal radiation}, \end{aligned}\right\} \tag{20}$$

The dimensionless form of skin drag force and Nusselt number are expressed as

$$\left.\begin{aligned} (\mathrm{Re}_x)^{\frac{1}{2}} C_f &= \left[f''(0) + \tfrac{n-1}{d}(We)^d (f'')^{d+1}\right] \\ -(\mathrm{Re}_x)^{-\frac{1}{2}} Nu_x &= (1+R)\theta'(0). \end{aligned}\right\} \tag{21}$$

5: Numerical solution

Here we consider steady, incompressible, two-dimensional mixed convective entropy optimized flow of Carreau-Yasuda fluid with Soret and Dufour effects towards a stretched surface of sheet. The nonlinear flow expression is first altered to ordinary differential equations through appropriate similarity transformation. The final system of ordinary ones is further altered into first order ODEs by introducing new variables and then tackled by Built-in-Shooting technique. The first order ordinary differential equations are

$$\left.\begin{aligned} f = y_1,\ \tfrac{df}{d\eta} = y_2,\ \tfrac{d^2 f}{d\eta^2} = y_3,\ \tfrac{d^3 f}{d\eta^3} = y_3' = yy_1, \\ \theta = y_4,\ \tfrac{d\theta}{d\eta} = y_5,\ \tfrac{d^2\theta}{d\eta^2} = y_5' = yy_2, \\ \phi = y_6,\ \tfrac{d\phi}{d\eta} = y_7,\ \tfrac{d^2\phi}{d\eta^2} = y_7' = yy_3. \end{aligned}\right\} \tag{22}$$

After implementing the above equation, the dimensionless Eqs. (11-13) with boundary conditions (14) take the form

$$\left.\begin{aligned} y_3' &= \left[\frac{d}{d+(We)^d (y_3)^d (n-1)(d+1)}\right]\left(y_2^2 - y_1 y_3 + \beta_1 y_2 - \lambda y_4 - N\lambda y_6\right), \\ y_5' &= -\left[\tfrac{1}{1+R}\right]\left(\Pr Ec\left((We)^d \tfrac{(n-1)}{d}(y_3)^d + 1\right) y_3^2 - \Pr y_1 y_5 - D_f \Pr y y_3\right), \\ y_7' &= -\left(LeSryy_2 + Ley_1 y_7 - Sc(1+\delta y_4)^m k_1 \exp\left[\tfrac{-E_1}{(1+\delta y_4)}\right]\right), \end{aligned}\right\} \quad (23)$$

with

$$\left.\begin{aligned} y_1(0) = 0,\ y_2(0) - 1 = 0,\ y_2(\infty) = 0, \\ y_5(0) + B_1(1 - y_4(0)) = 0,\ y_7(0) + B_2(1 - y_6(0)) = 0, \\ y_4(\infty) = 0,\ y_6(\infty) = 0. \end{aligned}\right\} \quad (24)$$

Numerical solutions of Eq. (23) with boundary condition (24) are solved through Built-in-Shooting method and the results are compared with published ones and finds very good agreement with them.

6: Results and discussion

This section is fully devoted to analyze the behavior of embedded parameters against velocity $\left(f'(\eta)\right)$, temperature $\left(\theta(\eta)\right)$, concentration $\left(\phi(\eta)\right)$, entropy generation $\left(N_G(\eta)\right)$ and Bejan number $\left(Be(\eta)\right)$ (see Figs. (1-16)).

Figs. (1-4) are sketched for behavior of velocity profile against Weissenberg number (We), magnetic parameter (β_1), mixed convection parameter (λ) and buoyancy ratio parameter (N_1). Fig. 1 reveals the influence of (We) against velocity field. Here velocity of the fluid is shown to be increasing for higher values (We). By definition of (We) we can see that viscosity is inversely related to it. So with increase in the values of (We) decays the viscosity (internal resistance to flow) of the fluid. Therefore, we can conclude that for higher $(We = 0, 0.7, 1.4, 2.1, 2.8)$ motion of the fluid rises. Fig. 2 is to show the impact of magnetic parameter against $\left(f'(\eta)\right)$. Here we see

that motion of the fluid slows down with increase in (β_1). Magnetic parameter is increasing function of Lorentz force (resistive force). Due to increase in resistive force fluid particles slows down and $(f'(\eta))$ decreases. Fig. 3 deals with mixed convection impact on $(f'(\eta))$. Velocity of the fluid enhances for greater values of λ. Since mixed convection parameter is ratio of buoyancy to viscous forces. With increase in values of (λ) buoyancy force rises due to which $(f'(\eta))$ increases. Impact of ratio of buoyancy forces parameter (N_1) on velocity field is shown in Fig. 4. Here $(f'(\eta))$ enhances for rising values of $(N_1 = 0, 0.7, 1.4, 2.1, 2.8)$. Fig. 5 tells the impact of Prandtl number (Pr) against temperature field $(\theta(\eta))$. Here temperature of the fluid decays for higher values of Prandtl number (Pr). Prandtl number is ratio between momentum diffusivity to thermal diffusivity. With increase in (Pr) thermal diffusivity decays due to which temperature of the fluid reduces. Fig. 6 describe the trend of $(\theta(\eta))$ against Eckert number (Ec). Total internal energy of the system enhances with increase in (Ec) due to which $(\theta(\eta))$ rises. Figs. 7 and 8 show the behavior of Dufour number (D_f) and thermal Biot number (B_1) against temperature field $(\theta(\eta))$. There is increase in $(\theta(\eta))$ for higher values of (D_f) and (B_1). Mass concentration gradient in energy field is responsible for Dufour effect because there is coupled effect of irreversible process. Due to which energy flux of the system enhances. Therefore, it increases the $(\theta(\eta))$ of the flow system (See Fig. 7). Fig. 9 shows the impact of Lewis number against concentration field and it is witnessed that concentration of the fluid is decreasing. With increasing (Le) mass diffusivity decreases due to which mass concentration also decays. Fig. 10 is constructed to analyze the behavior of (Sr) via $(\phi(\eta))$. Here concentration of the fluid enhances

against Soret number. Due to impact of irreversible process temperature gradient in the concentration field Soret effect generates. It has the capability to enhance the concentration flux of the flow system. Therefore, we can conclude that due to this concentration of the fluid enhances. Figs. 11 and 12 explain the trend of $(\phi(\eta))$ against activation energy parameter and solutal Biot number. $(\phi(\eta))$ is increasing function of both parameters. Increasing activation energy parameter with less temperature, consequences lower constant reaction rate then small reaction is practiced. This enhances the solute of concentration (see Fig. 11). Figs. 13 and 14 depict the influence of Brinkman number (Br) on entropy generation (N_G) and Bejan number (Be). Viscosity of the fluid is increasing function of Brinkman number by definition. So when we increase the values of Br viscous dissipation irreversibility enhances due to which more disturbance occur between the system and consequently (N_G) increases (see Fig. 13). Fig. 14 reveals that Bejan number is decreasing function of Br because viscous dissipation irreversibility is dominant over heat and mass transfer irreversibility (See Fig. 14). Figs. 15 and 16 show the impact of Weissenberg number (We) against (N_G) and Bejan number (Be). It also shows that entropy of the fluid is more for greater estimations of (We) while opposite behavior is seen for Bejan number.

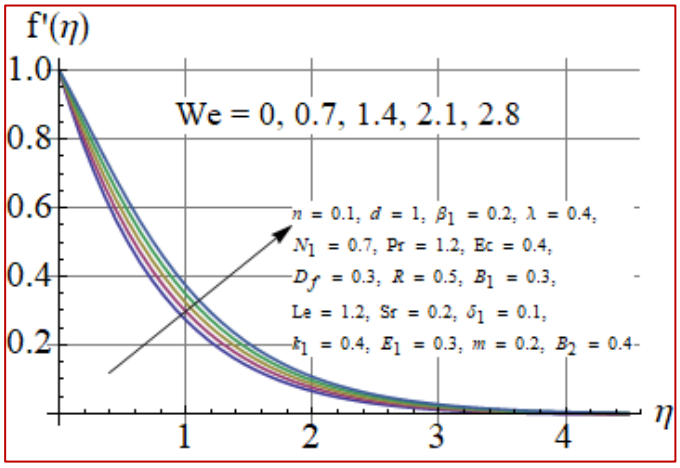

Fig. 1: Impact of Weissenberg number on velocity

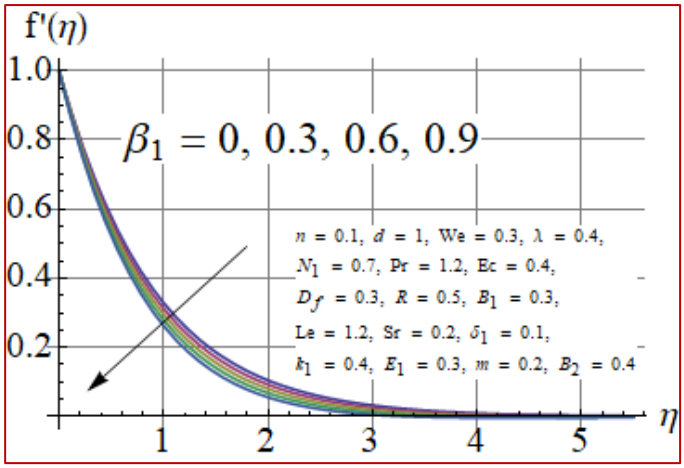

Fig. 2: *Impact of magnetic parameter on velocity*

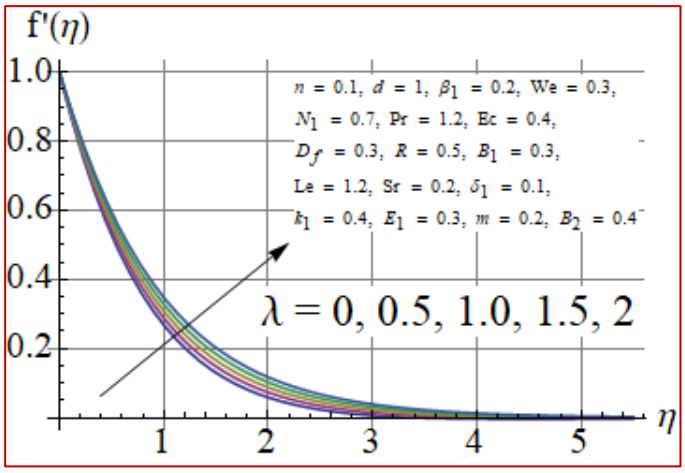

Fig. 3: *Impact of mixed convection parameter on velocity*

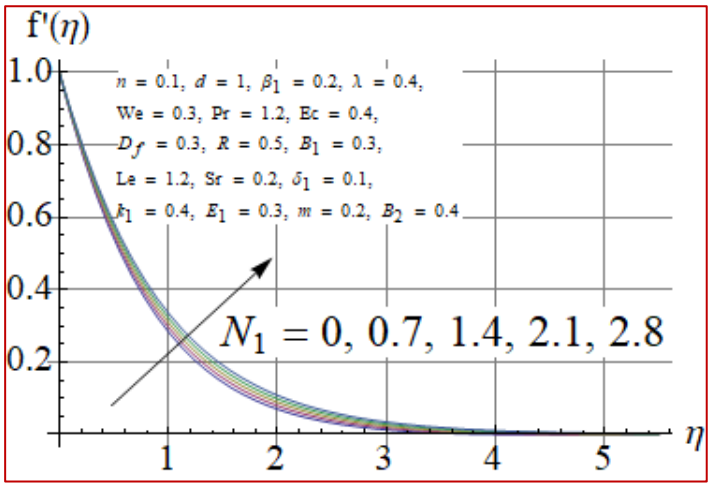

Fig. 4: *Impact of* buoyancy ratio parameter *on velocity*

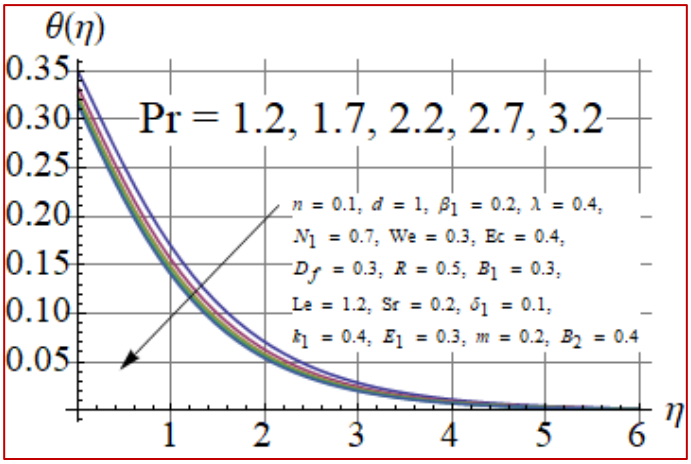

Fig. 5: *Impact of* Prandtl number *on temperature*

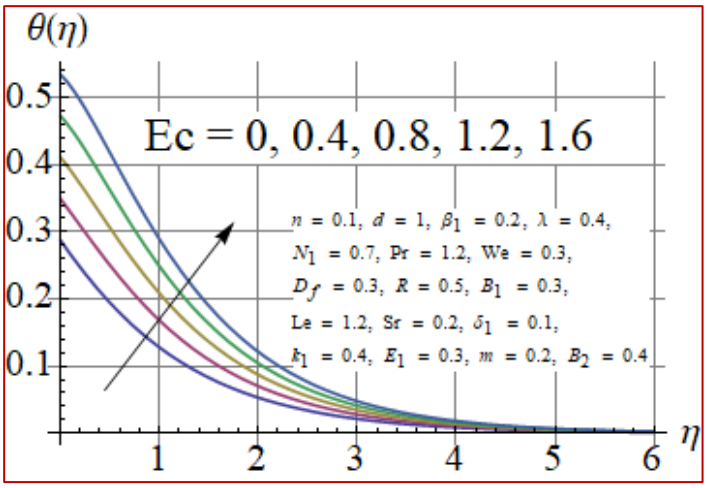

Fig. 6: *Impact of* Eckert number *on temperature*

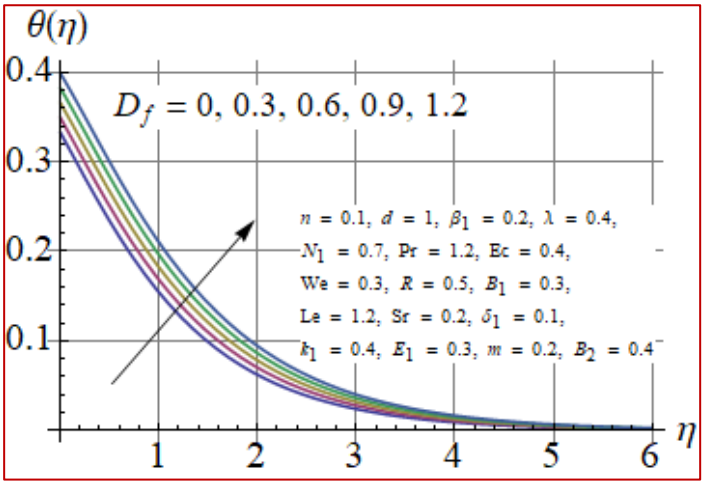

Fig. 7: *Impact of* Dufour number *on temperature*

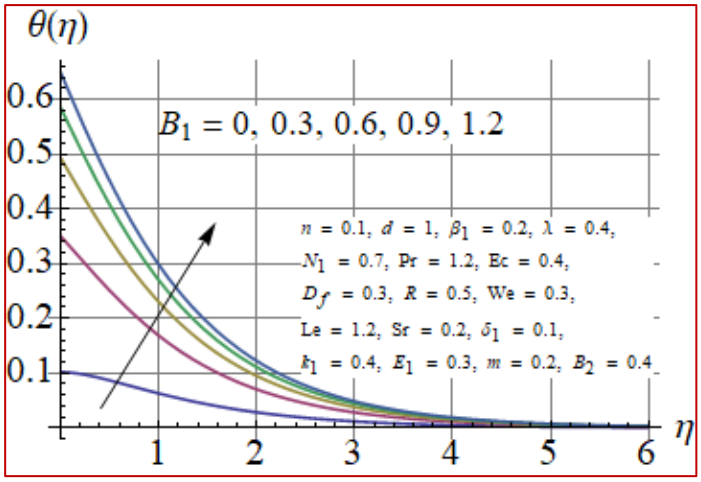

Fig. 8: *Impact of* thermal Biot number *on temperature*

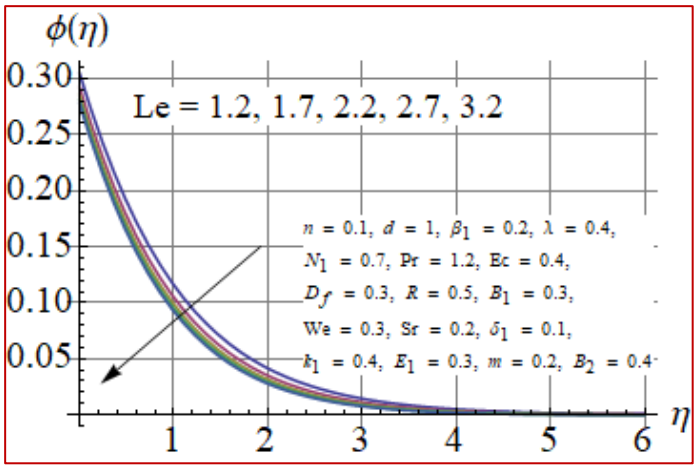

Fig. 9: *Impact of* Lewis number *on concentration*

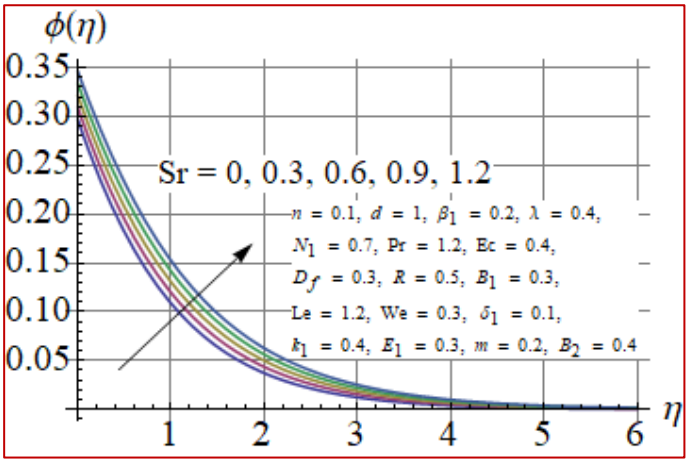

Fig. 10: *Impact of* Soret number *on concentration*

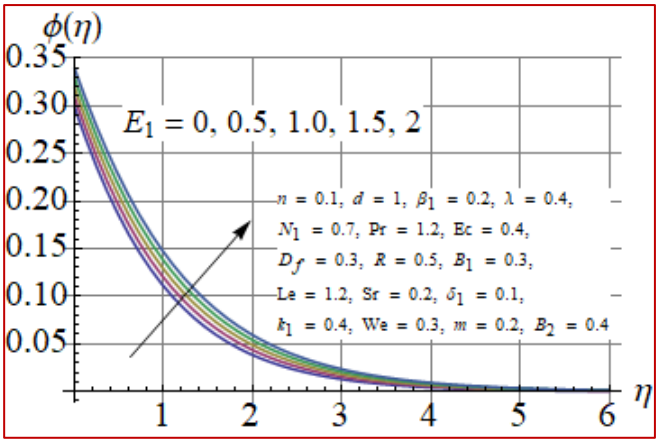

Fig. 11: *Impact of* activation energy parameter *on concentration*

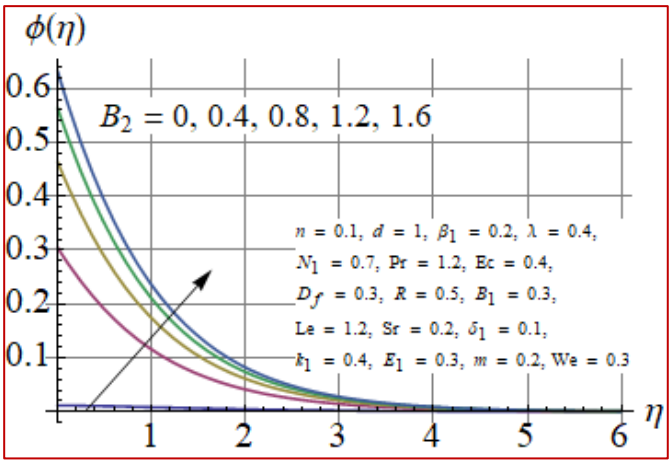

Fig. 12: *Impact of* Solutal Biot number *on concentration*

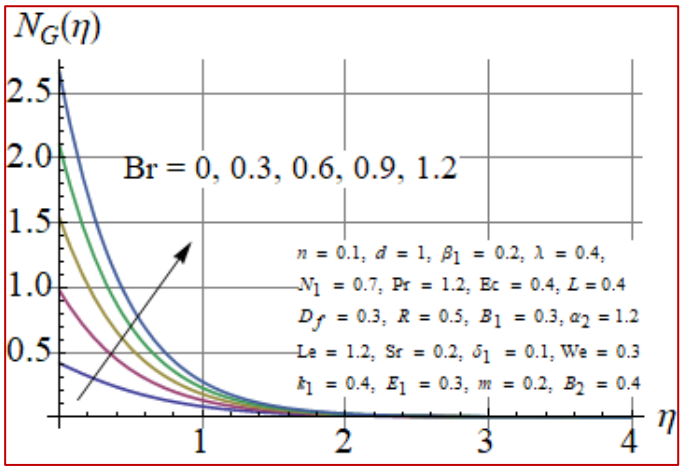

Fig. 13: *Impact of* Brinkman number *on entropy generation rate*

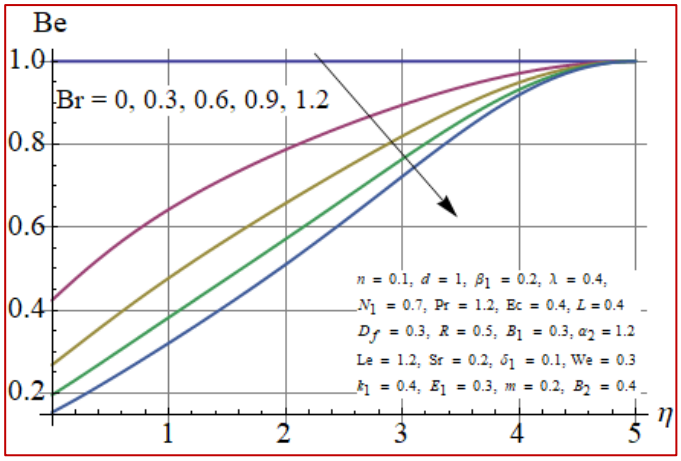

Fig. 14: *Impact of* Brinkman number *on Bejan number*

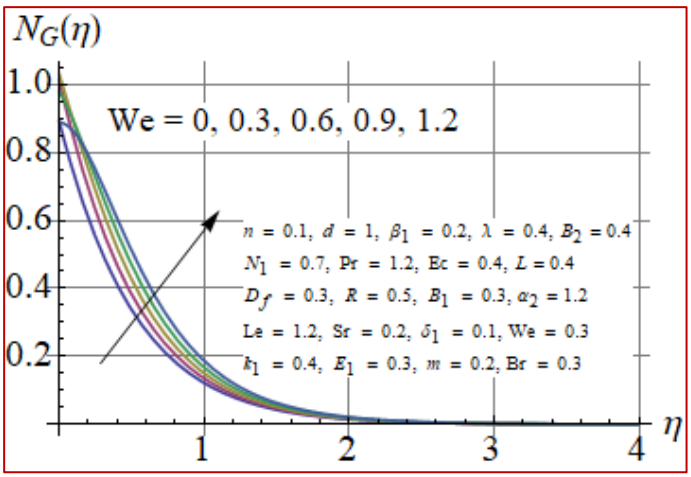

Fig. 15: *Impact of* Weissenberg number *on entropy generation rate*

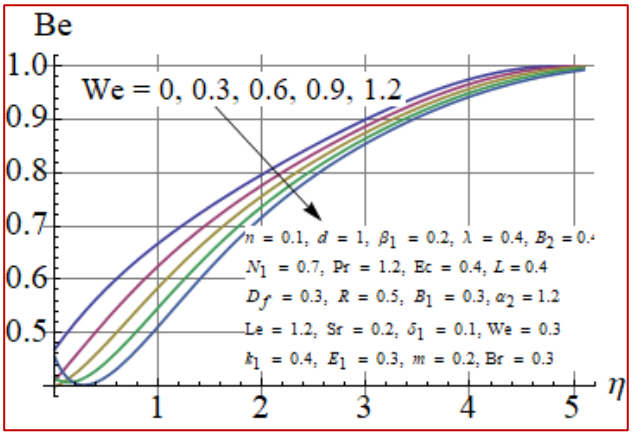

Fig. 16: *Impact of* Weissenberg number *on Bejan number*

7: Physical quantities

In this section we will discuss the impact of embedded parameters against skin friction and Nusselt number (See Table 1 and 2). Table shows that surface drag force rises with increasing values of mixed convection parameter and magnetic parameter while opposite trend is seen for Weissenberg number. Table 2 elaborates the influence of Prandtl number, Dufour number and Eckert number via Nusselt number. Heat transfer rate enhances for Pr on the other hand decreases for D_f and Ec. Table 3 shows that in the limiting case our problem shows the good agreement with the previous published literature. Here we have compared our results of $f''(0)$ with [41], [42] and [43] in limiting case and we found an excellent agreement which proofs the validity of our problem.

Table 1: Skin friction values under variation of relevant variables.

λ	We	β_1	$-\mathrm{Re}_x^{1/2} C_f$
1	0.1	0.2	0.9430
2			0.9474
3			0.9532
1	0.2		0.9387
	0.3		0.9344
	0.4		0.9283
	0.1	0.4	1.0050
		0.6	1.0740
		0.8	1.1210

Table 2: Nusselt number values under variation of relevant variables.

Pr	D_f	Ec	$\mathrm{Re}_x^{1/2}\, Nu_x$
1.0	0.3	0.5	1.1300
1.1			1.2180
1.2			1.2921
1.0	0.4		1.0131
	0.5		0.9086
	0.6		0.8037
	0.3	0.6	1.0220
		0.7	0.9230
		0.8	0.8217

Table 3: Comparison of $f''(0)$ with [41], [42] and [43] when $We = \lambda = N_1 = 0, d = n = 1$.

β_1	Akber et al. [41]	Bilal et al. [42]	Fatehzadeh et at. [43]	Present
0	-1.000	-1.000	-1.000	-1.000
0.5	1.11803	1.11800	---	1.11801
1.0	-1.41419	-1.41421	-1.41421	-1.4142

8: Conclusions

Major findings of this research are:

- (f') enhances via λ, We and N_1 while opposite trend is seen for magnetic parameter.
- Temperature of the fluid rises by enhancing (B_1) and (D_f).
- Concentration is increasing function of (E_1) and (Sr).

- Entropy of the system enhances for higher (Br) and (We).
- Bejan number have inverse relation with (Br) and (We).

References

[1] R. Bird, Non-Newtonian behavior of polymeric liquids, Physica A: Statistical Mechanics and its Applications, 118 (1983) 3-16.

[2] R. P. Chhabra and J .F. Richardson, Non-newtonian flow and applied rheology (2nd Ed.) (2008).

[3] R. Mahmood, S.Bilal, I. Khan, N. Kousar, A. H.Seikh, El-Sayed M. Sherif, A comprehensive finite element examination of Carreau Yasuda fluid model in a lid driven cavity and channel with obstacle by way of kinetic energy and drag and lift coefficient measurements, Journal of Materials Research and Technology, 9 (2020) 1785-1800.

[4] T. Sochi and M. J. Blunt, Pore-scale network modeling of Ellis and Herschel--Bulkley fluids, Journal of Petroleum Science and Engineering, 60 (2008) 105-124.

[5] S. Xun, J. Zhao, L. Zheng, X. Chen and X. Zhang, Flow and heat transfer of Ostwald-de Waele fluid over a variable thickness rotating disk with index decreasing, International Journal of Heat and Mass Transfer, 103 (2016) 1214-1224.

[6] S. Qayyum, M.I. Khan, T. Hayat, A. Alsaedi and M. Tamoor, Entropy generation in dissipative flow of Williamson fluid between two rotating disks, International Journal of Heat and Mass Transfer, 127 (2018) 933-942.

[7] M. I. Khan, T. Hayat, M.I. Khan and A. Alsaedi, Activation energy impact in nonlinear radiative stagnation point flow of Cross nanofluid, International Communications in Heat and Mass Transfer, 91 (2018) 216-224.

[8] M. I. Khan, S. Afzal, T. Hayat, M. Waqas and A. Alsaedi, Activation energy for the Carreau-Yasuda nanomaterial flow: Analysis of the entropy generation over a porous medium, Journal of Molecular Liquids, 297 (2020) 111905.

[9] M. Waqas, M.I. Khan, T. Hayat and A. Alsaedi, Numerical simulation for magneto Carreau nanofluid model with thermal radiation: A revised model, Computer Methods in Applied Mechanics and Engineering, 324 (2017) 640-653.

[10] L.C.F. Andrade, The Carreau-Yasuda Fluids: a skin friction equation for turbulent flow in pipes and Kolmogorov dissipative scales, Journal of the Brazilian Society of Mechanical Sciences and Engineering, 29 (2007) 162-167.

[11] G. R. Kefayati and H. Tang, Three-dimensional Lattice Boltzmann simulation on thermosolutal convection and entropy generation of Carreau-Yasuda fluids, International Journal of Heat and Mass Transfer, 131 (2019) 346-364.

[12] T. Hayat, M.I. Khan, M. Farooq, A. Alsaedi, M. Waqas and T. Yasmeen, Impact of Cattaneo-Christov heat flux model in flow of variable thermal conductivity fluid over a variable thicked surface, International Journal of Heat and Mass Transfer 99 (2016) 702-710.

[13] M. I Khan, M. Waqas, T. Hayat, A. Alsaedi, A comparative study of Casson fluid with homogeneous-heterogeneous reactions, Journal of Colloid and Interface Science, 498 (2017) 85-90.

[14] N. S. Elgazery and A. F. Elelamy, Multiple solutions for non-Newtonian nanofluid flow over a stretching sheet with nonlinear thermal radiation: Application in transdermal drug delivery, Pramana, 94 (2020) 68.

[15] S. Ghosh and S. Mukhopadhyay, MHD mixed convection flow of a nanofluid past a stretching surface of variable thickness and vanishing nanoparticle flux, Pramana, 94 (2020)

61.

[16] P. J. Carreau, Rheological equations from molecular network theories, Transactions of the Society of Rheology, 16 (1972) 99-127.

[17] K. Yasuda, Investigation of the analogies between viscometric and linear viscoelastic properties of polystyrene fluids, PhD Thesis. Massachusetts Institute Technology, Department of Chemical Engineering, 1979.

[18] B. C. Sakiadis, Boundary-layer behaviour on continuous solid surfaces: I. Boundary layer equations for two-dimensional and axisymmetric flow, American Institute of Chemical Engineers, 7 (1961) 26-28.

[19] L. J. Crane, Flow past a stretching plate, Zeitschrift für angewandte Mathematik und Physik (ZAMP), 21 (1970) 645-647.

[20] E. Magyari and B. Keller, Exact solutions for self-similar boundary-layer flows induced by permeable stretching walls, European Journal of Mechanics-B/Fluids 19 (2000) 109-122.

[21] A. Ishak, R. Nazar and I. Pop, Boundary layer flow and heat transfer over an unsteady stretching vertical surface, Meccanica 44 (2009) 369-375.

[22] M. Rashid, T. Hayat, K. Rafique and A. Alsaedi, Chemically reactive flow of thixotropic nanofluid with thermal radiation, Pramana 93 (2019) 97.

[23] K. L. Hsiao. Combined electrical MHD heat transfer thermal extrusion system using Maxwell fluid with radiative and viscous dissipation effects, Applied Thermal Engineering, 112 (2017) 1281-1288.

[24] M.I. Khan, T. Hayat, M.I. Khan, M. Waqas and A. Alsaedi, Numerical simulation of hydromagnetic mixed convective radiative slip flow with variable fluid properties: A mathematical model for entropy generation, Journal of Physics and Chemistry of Solids, 125

(2019) 153-164.

[25] S. I. Abdelsalam and M. Sohail, Numerical approach of variable thermophysical features of dissipated viscous nanofluid comprising gyrotactic micro-organisms, Pramana, 94 (2020) (2020).

[26] T. Hayat, M.I. Khan, M. Farooq, N. Gull and A. Alsaedi, Unsteady three-dimensional mixed convection flow with variable viscosity and thermal conductivity, Journal of Molecular Liquids, 223 (2016) 1297-1310.

[27] P. Mathur and S. R. Mishra, Free convective Poiseuille flow through porous medium between two infinite vertical plates in slip flow regime, Pramana, 94 (2020) 69.

[28] S.Z. Abbas, W.A. Khan, S. Kadry, M.I. Khan, M. Waqas and M.I. Khan, Entropy optimized Darcy-Forchheimer nanofluid (silicon dioxide, molybdenum disulfide) subject to temperature dependent viscosity, Computer Methods and Programs in Biomedicine, 190 (2020) 105363.

[29] S. Z. Abbas, M.I. Khan, S. Kadry, W.A. Khan, M. Israr-Ur-Rehman and M. Waqas, Fully developed entropy optimized second order velocity slip MHD nanofluid flow with activation energy, Computer Methods and Programs in Biomedicine, 190 (2020) 105362.

[30] B. Ramadevi, K. A. Kumar, V. Sugunamma and N. Sandeep, Influence of non-uniform heat source/sink on the three-dimensional magnetohydrodynamic Carreau fluid flow past a stretching surface with modified Fourier's law, Pramana. 93 (2019) 86.

[31] J. Wang, M.I. Khan, W.A. Khan, S.Z. Abbas and M.I. Khan, Transportation of heat generation/absorption and radiative heat flux in homogeneous--heterogeneous catalytic reactions of non-Newtonian fluid (Oldroyd-B model), Computer Methods and Programs in Biomedicine, 189 (2020) 105310.

[32] R. Muhammad, M.I. Khan, N.B. Khan and M. Jameel, Magnetohydrodynamics (MHD) radiated nanomaterial viscous material flow by a curved surface with second order slip and entropy generation, Computer Methods and Programs in Biomedicine, 189 (2020) 105294.

[33] A. Bejan, Entropy generation minimization, 2nd ed. Boca Raton: CRC; 1996.

[34] M. M. Rashidi, S. Abelman, N. Freidoonimehr, Entropy generation in steady MHD flow due to a rotating porous disk in a nanofluid, International Journal of Heat and Mass Transfer, 62 (2013) 515-25.

[35] M. M. Rashidi, N. Kavyani and S. Abelman, Investigation of entropy generation in MHD and slip flow over a rotating porous disk with variable properties, International Journal of Heat and Mass Transfer, 70 (2014) 892-917.

[36] A. Malvandi, D. D. Ganji, F. Hedayati, R. E. Yousefi, An analytical study on entropy generation of nanofluids over a flat plate, Alexandria Engineering Journal, 52 (2013) 595-604.

[37] A. Soraya and S. Salah, Second law analysis of viscoelastic fluid over a stretching sheet subject to a transverse magnetic field with heat and mass transfer, Entropy, 12 (2010) 1867-1884.

[38] H. Sardar, L. Ahmad, M. Khan and A. S. Alshomrani, Investigation of mixed convection flow of Carreau nanofluid over a wedge in the presence of Soret and Dufour effects, International Journal of Heat and Mass Transfer, 137 (2019) 809-822.

[39] G. K. Ramesh, Analysis of active and passive control of nanoparticles in viscoelastic nanomaterial inspired by activation energy and chemical reaction, Physica A: Statistical Mechanics and its Applications, 55015 (2020) 123964.

[40] F. Mabood, W. A. Khan and M. M. Yovanovich, Forced convection of nanofluid flow across horizontal circular cylinder with convective boundary condition, Journal of Molecular

Liquids, 222 (2016) 172-180.

[41] N. S. Akbar, A. Ebaid and Z. H. Khan, Numerical analysis of magnetic field effects on Eyring-Powell fluid flow towards a stretching sheet. Journal of Magnetism and Magnetic Materials, 382 (2015) 355-358.

[42] S. Bilal, M. Y. Malik, M. Awais, K. U. Rehman, A. Hussain and M. I. Khan, Numerical investigation on 2D viscoelastic fluid due to exponentially stretching surface with magnetic effects: an application of non-Fourier flux theory. Neural Computing and Applications, 30 (2018) 2749-2758.

[43] M. Fathizadeh, M. Madani, Y. Khan, N. Faraz, A. Yildirim and S. Tutkun, An effective modification of the homotopy perturbation method for MHD viscous flow over a stretching sheet. Journal of King Saud University-Science, 25 (2013) 107-113.